

Pressure-less joining materials for SiC-based components for light water reactors

*Original*

Pressure-less joining materials for SiC-based components for light water reactors / Ferraris, M., La Pierre, S.D., Casalegno, V., Bosch, R., Marrow, J., Chen, Y., Bourlet, F., Lorrette, C., Huang, S., Lambrinou, K.. - In: OPEN CERAMICS. - ISSN 2666-5395. - 25:(2026). [10.1016/j.oceram.2025.100886]

*Availability:*

This version is available at: 11583/3005373 since: 2025-11-24T13:16:44Z

*Publisher:*

Elsevier

*Published*

DOI:10.1016/j.oceram.2025.100886

*Terms of use:*

This article is made available under terms and conditions as specified in the corresponding bibliographic description in the repository

*Publisher copyright*

(Article begins on next page)



## Pressure-less joining materials for SiC-based components for light water reactors

Monica Ferraris<sup>a,\*</sup>, Stefano De la Pierre<sup>a</sup>, Valentina Casalegno<sup>a</sup>, Rik-Wouter Bosch<sup>b</sup>, James Marrow<sup>c</sup>, Yang Chen<sup>c</sup>, Frédérique Bourlet<sup>d</sup>, Christophe Lorrette<sup>d</sup>, Shuigen Huang<sup>e</sup>, Konstantina Lambrinou<sup>f</sup>

<sup>a</sup> Politecnico di Torino and J-Tech@PoliTO, Torino 10129, Italy

<sup>b</sup> SCK CEN, Boeretang 200, Mol 2400, Belgium

<sup>c</sup> Department of Materials, University of Oxford, Parks Rd, Oxford, OX1 3PH, UK

<sup>d</sup> Université Paris-Saclay, CEA, Service de Recherche en Matériaux et procédés Avancés, F91191 Gif-sur-Yvette, France

<sup>e</sup> Department of Materials Engineering, KU Leuven, Kasteelpark Arenberg 44, Leuven 3001, Belgium

<sup>f</sup> School of Computing and Engineering, University of Huddersfield, Queensgate, Huddersfield HD1 3DH, UK

### ARTICLE INFO

#### Keywords:

Joining  
Pressure-less  
LWR  
Glass-ceramics

### ABSTRACT

Silicon carbide fiber-reinforced composites (SiC/SiC) are leading candidates to replace zirconium-based alloys as cladding in light water reactors (LWR), owing to their exceptional oxidation resistance and mechanical performance under accident conditions.

However, pressure-less joining methods compatible with the extreme chemical and thermal environment of LWRs remain a major technological hurdle.

This work evaluates two promising joining materials—Mo-wrap (a MoSi<sub>2</sub>/Si composite) and SAY (a silica–alumina–yttria glass-ceramic)—under simulated LWR conditions.

Joining was performed using both conventional furnaces and laser-assisted techniques.

Joint integrity and microstructure were assessed by SEM/EDS and X-ray computed tomography. Hydrothermal stability was evaluated in static and flowing-water (loop) autoclaves up to 30 days at 330 °C and 150–155 bar.

Mo-wrap joints showed partial degradation due to silicon dissolution, while SAY joints retained good structural integrity in static tests but suffered phase-selective corrosion under flowing conditions, with keivite emerging as the most stable crystalline phase.

Laser-processed amorphous SAY joints exhibited improved corrosion resistance, though still limited under prolonged exposure.

These findings advance the understanding of joining performance in nuclear-relevant environments and support the development of accident-tolerant fuel cladding.

### 1. Introduction

Zirconium-based (Zr) alloys have served as light-water-reactor (LWR) fuel cladding for decades, yet the Fukushima-Daiichi accident exposed their main vulnerability: in high-temperature steam they oxidize rapidly, releasing large amounts of hydrogen and intensifying heat generation. Global research therefore focuses on accident-tolerant materials that react more slowly with steam and suppress hydrogen production [1,2].

Continuous-fibre silicon-carbide composite (SiC/SiC) cladding is a

leading candidate. It exhibits negligible oxidation in 1000 °C steam, does not generate hydrogen, and retains mechanical integrity under loss-of-coolant scenarios [2]. A practical hurdle, however, is sealing the four-metre SiC/SiC tubes after fuel loading: unlike Zr alloys, SiC/SiC cannot be fusion-welded.

Several joining technologies and materials for SiC/SiC have been proposed [3], only a few have been tested in nuclear-relevant environments [4–7] and even less in LWR conditions [8,9].

Methods that combine heat with external pressure (e.g. hot-pressing) face scale-up challenges and high capital cost. Pressure-less techniques

\* Corresponding author.

E-mail address: [monica.ferraris@polito.it](mailto:monica.ferraris@polito.it) (M. Ferraris).

<https://doi.org/10.1016/j.oceram.2025.100886>

Received 13 October 2025; Received in revised form 13 November 2025; Accepted 18 November 2025

Available online 19 November 2025

2666-5395/© 2025 The Author(s). Published by Elsevier Ltd on behalf of European Ceramic Society. This is an open access article under the CC BY-NC-ND license (<http://creativecommons.org/licenses/by-nc-nd/4.0/>).

are therefore preferred: they permit inexpensive furnace or localised-laser heating [10] and can accommodate long, thin-walled components.

Successful pressure-less joining materials for SiC/SiC for LWR application hinges on a joining material compatible with *both* SiC chemistry and LWR service.

One excellent way to have both is based on the choice of SiC itself as joining material: this achievement has been very recently described by General Atomics [11]; the patented, localized SiC-based joining method is an engineered, multilayer composite cladding structure successfully verified for irradiation resistance at the Oak Ridge National Laboratory High Flux Isotope Reactor test reactor. Now, it is under testing to evaluate the quality of these joints under high temperature, high pressure, and corrosive water coolant environment expected in pressurized water reactors. Now, joints remain gas-tight after 180-days of exposure in Westinghouse's reactor coolant test facility.

Other current options—glass, glass-ceramic, and active-metal brazes—still exhibit the major drawback of unknown behavior in relevant LWR conditions. Thus, a fully suitable joining system for SiC/SiC LWR cladding remains of potential interest.

This study evaluates two potentially LWR compatible pressure-less joining materials:

- **Mo-wrap**—a molybdenum-disilicide/silicon (MoSi<sub>2</sub>/Si) composite produced by wrapping Si foils in a Mo sheet and reacting above the Si melting point. The process prevents molten Si outflow, is highly adaptable, and yields joints with ~50 MPa lap-shear strength at 1000 °C [12–15].
- **SAY glass-ceramic**—a silica–alumina–yttria composition that crystallises to mullite, cristobalite, and keivite on cooling. SAY shows thermal-expansion compatibility with SiC, good wettability, and proven resistance to neutron and heavy-ion irradiation up to ≈ 40 dpa without amorphisation or strength loss [4,6,7,16–18].

Joints were fabricated on SiC/SiC tubes using both furnace heating and laser-assisted local joining. Internal integrity was assessed by X-ray computed tomography at Oxford University (UK) and J-Tech@PoliTO, Politecnico di Torino (Italy).

Hydrothermal stability was then tested in static and flowing-water autoclaves that replicate LWR primary-loop conditions.

The results presented here clarify the suitability of Mo-wrap and SAY glass-ceramic for sealing SiC/SiC cladding and advance the development of accident-tolerant fuel systems.

## 2. Experimental

### 2.1. Materials

#### 2.1.1. SiC and SiC-based composites

Preliminary tests were conducted on monolithic silicon carbide (SiC) samples (density: 3.1 g/cm<sup>3</sup>; purity: 98.5 %), supplied by Bettini S.p.A. (Italy). Subsequent experiments were carried out on SiC/SiC composite materials.

The SiC/SiC composites were produced via Chemical Vapor Infiltration (CVI) and supplied by the French Alternative Energies and Atomic Energy Commission (CEA). They were reinforced with third-generation Hi-Nicalon™ Type S SiC fibers, selected for their proven performance in nuclear environments. The same fiber and CVI process were used to fabricate both the cladding tubes and the end plugs.

Cladding tubes (length: 50 mm) were manufactured by filament winding of three fiber layers at ±45° orientation. Before matrix infiltration, the fiber surfaces were coated with approximately 50 nm of pyrolytic carbon (PyC). Densification of the SiC matrix was then performed using the CVI method. Final machining (internal and external grinding) ensured tight dimensional tolerances: an inner diameter of 7.92 ± 0.02 mm and an outer diameter of 9.67 ± 0.01 mm.

End plugs were similarly ground and polished to meet dimensional

specifications and ensure compatibility with the joining procedures. A schematic of the end plug geometries (Type 1 and Type 2), along with the closed tube configuration, is shown in Fig. 1. Further details on the fabrication of the SiC/SiC components are available in reference in references [19–21].

#### 2.1.2. Mo-wrap joining

The Mo-wrap process involves enclosing silicon foils within a wrap of refractory metal—molybdenum, in this work—to prevent molten silicon from leaking during the joining process. This containment avoids infiltration into the substrates and enables controlled bonding. Upon heating, an in-situ composite forms: a silicon matrix reinforced by molybdenum disilicide (MoSi<sub>2</sub>) phases [12–15].

Mo-wrap was employed in this work to coat and join monolithic SiC. The optimized protocol consisted of heating to 1450 °C at a rate of 1000 °C/h, followed by a 10-minute dwell at peak temperature in an inert argon atmosphere.

#### 2.1.3. SAY glass-ceramic joining

The preparation and application of SAY (silica–alumina–yttria) glass as a joining material for SiC/SiC have been reported previously [4,6,7,16–18] and are briefly summarized here.

SAY glass was synthesized by melting a batch of SiO<sub>2</sub> (54 wt. %), Al<sub>2</sub>O<sub>3</sub> (18.07 wt. %), and Y<sub>2</sub>O<sub>3</sub> (27.93 wt. %) in a Pt–Rh crucible at 1450 °C for 1 h in a Carbolite furnace, followed by quenching on a cold plate to form a homogeneous glass.

Thermal characterization was carried out by differential dilatometry (DIL 402 PC, NETZSCH, Germany) and heating-stage microscopy (Hesse Instruments, Harzgerode, Germany), equipped with an image analysis system (EM 301, Hesse Instruments).

Measurements at a heating rate of 10 °C/min gave the following characteristic temperatures: glass transition temperature T<sub>g</sub> = 910 °C, crystallization onset T<sub>x</sub> = 1235 °C, and melting temperature T<sub>m</sub> = 1375 °C.

The coefficient of thermal expansion (CTE) of the as-cast glass was measured as 3.8 × 10<sup>-6</sup> °C<sup>-1</sup> (400–700 °C). After controlled crystallization (T<sub>x</sub> = 1235 °C, 1 hour), the resulting glass-ceramic exhibited a CTE of 5.5 × 10<sup>-6</sup> °C<sup>-1</sup> in the same temperature range.

Thermal stability was assessed up to 1300 °C in accordance with standard as reported in [10].

Phase composition after crystallization was determined by X-ray diffraction (Malvern PANalytical X'Pert PRO), using X'Pert HighScore software. The as-cast glass was fully amorphous, while the crystallized product consisted of mullite, cristobalite, and keivite phases.

For joining, the SAY glass was ground, sieved to <38 μm, and mixed with a minimal amount of isopropyl alcohol to form a slurry. This slurry was applied between the SiC/SiC components, which were then joined in a Nabertherm tubular furnace under argon flow. The thermal cycle included heating to 1450 °C (rate: 1000 °C/h) with a 20-minute dwell, followed by controlled cooling to 1235 °C and an additional 1-hour dwell to induce crystallization.

Laser-based joining using the same slurry was also performed at TU Dresden (Germany) under ambient air. The process parameters are reported in [22–25].

## 3. Characterizations

### 3.1. Autoclave testing under simulated LWR conditions

The joining materials were initially pre-screened for hydrothermal stability at Politecnico di Torino (POLITO) using a static autoclave system (High Pressure Chemical Reactor, 100 mL, Supercritical Fluid Technology). The test was conducted at 312–325 °C and 150 bar, with stirring at 60 rpm. The thermal cycle included a 45-minute ramp to dwell temperature, an 8-hour dwell, and a 30-minute cooling phase. The autoclave was filled with demineralized water containing 8–9 ppm

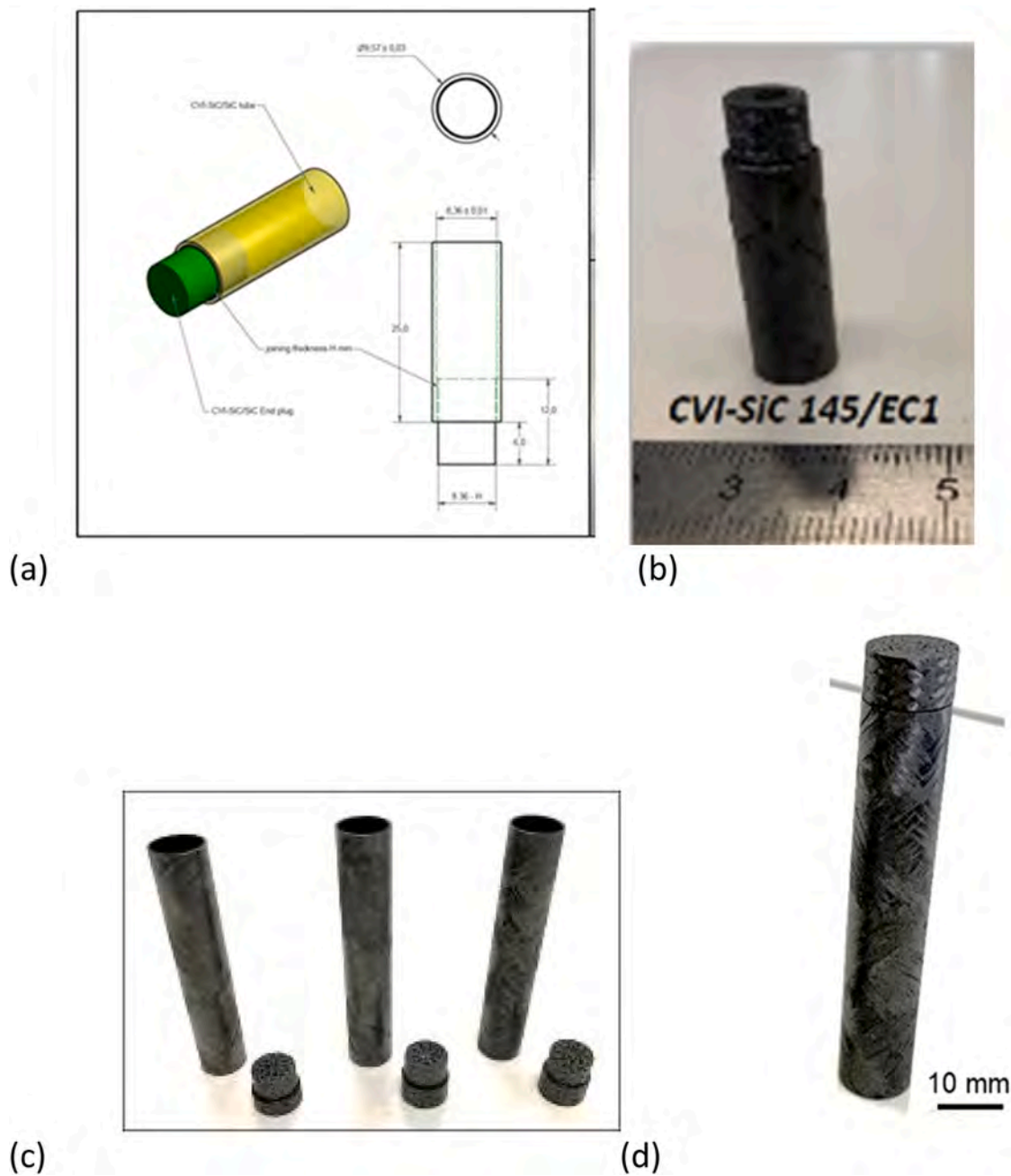


Fig. 1. Type 1 (a, b) and Type 2 (c,d) end plugs and joined samples.

dissolved oxygen.

Samples that passed this preliminary screening were subsequently tested at SCK • CEN, first in the PARR static autoclave and then in the CORTELINI forced-convection loop autoclave. The water chemistry, temperature, and pressure conditions used in these systems are summarized in Table I.

### 3.2. Static test (PARR, SCK•CEN)

Each specimen was placed in a stainless-steel basket and immersed in a static autoclave (PARR, 100 mL) operating at 330 °C (Fig. 2). The water chemistry replicated pressurised-water-reactor (PWR) primary coolant (1 000 ppm B as H<sub>3</sub>BO<sub>3</sub> and 2 ppm Li as LiOH) under an N<sub>2</sub> cover gas. Pressure was governed solely by the saturated-steam curve at the

Table I

Water chemistry, temperature, pressure and duration of tests in autoclaves.

Autoclave	Water chemistry	Cover gas	Temperature (°C)	Pressure (bar)	Test time
Static (POLITO)	8–9 ppm oxygen in demineralized water	N <sub>2</sub>	312–325	150	8 h
Static (PARR, SCK•CEN)	1000 ppm B, 2 ppm Li	N <sub>2</sub>	330	150	14 days
PWR loop (CORTELINI, SCK•CEN)	1000 ppm B, 2 ppm Li	45 mL/kg H <sub>2</sub>	330	155	30 days

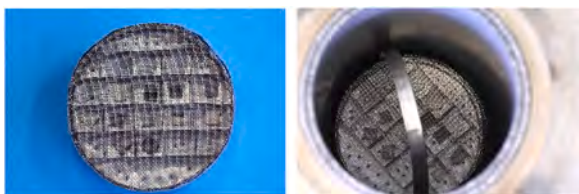


Fig. 2. Experimental arrangement of the test specimens for the static autoclave (PARR, SCK•CEN).

test temperature, so hydrogen chemistry could not be applied. These static tests served as a pre-selection step before flowing-loop exposure.

### 3.3. Flowing-loop tests (CORTELINI, SCK•CEN)

Specimens that passed the static screen were mounted in the CORTELINI forced-convection loop, where dissolved-hydrogen levels can be precisely controlled. Demineralised water containing  $H_3BO_3$ , LiOH, and  $H_2$  was recirculated at  $\sim 10 \text{ L h}^{-1}$ . After exiting the  $330 \text{ }^\circ\text{C}$  autoclave, the coolant was cooled to room temperature; conductivity, dissolved-oxygen, dissolved-hydrogen, and pH were monitored continuously, and samples were analysed before and after each run (Fig. 3).



Fig. 3. Experimental arrangement of the test specimens for the PWR loop (CORTELINI, SCK•CEN).

### 3.4. Post-exposure cleaning

All specimens were ultrasonically cleaned in ethanol for 15 min, then dried at  $100 \text{ }^\circ\text{C}$  for 30 minutes.

### 3.5. Microstructural examination

Fracture surfaces and cross-sections were investigated by SEM (JCM-6000Plus, JEOL) and by high-resolution FE-SEM (MERLIN Gemini II, ZEISS) equipped with EDX for elemental mapping.

### 3.6. X-ray computed tomography

Internal joint integrity—including porosity distribution and joining material homogeneity—was assessed by X-ray CT, with the two facilities whose characteristics are summarized in Table II.

## 4. Results and discussion

### 4.1. Mo-wrap

Based on previous results reported in more than two decades of activity [4,6,7,16–18], two pressureless joining materials - Mo-wrap and SAY - already demonstrated to be effective for bonding SiC and SiC-based composites were tested under simulated Light Water Reactor (LWR) conditions as summarized in Table I.

Fig. 4 shows a SEM-EDS cross-section of a Mo-wrap joined SiC sample (a) and a higher magnification of the joint region (b). As previously reported [12–15],  $MoSi_2$  particles are well embedded in the silicon matrix.

The stability of this material was initially evaluated in static autoclave tests (POLITO, 8 h, Table I) using Mo-wrap as a coating for SiC. Fig. 5 shows the surface morphology (SEM top view) of the Mo-wrap coating before (a) and after (b) the autoclave exposure, highlighting its unchanged morphology.

Following these promising results, Mo-wrap joined SiC samples were subjected to 14-day exposure in the PARR static autoclave at SCK•CEN (Table I). Fig. 6 (a–c) presents the outcomes. The samples remained joined after 14 days (b), although visible corrosion of the joining material was observed, especially in the central area. Fig. 6(c) shows  $MoSi_2$  particles retained within a residual silicon matrix. The dissolution of metallic silicon in LWR conditions was confirmed through testing of pure silicon slabs [26], which were completely dissolved after 14 days in the static autoclave.

To the best of the authors' knowledge, the behavior of pure metallic silicon under these autoclave conditions has not previously been reported. Only reference [27] mentions silicon dissolution, but in the context of NITE SiC/SiC composites exposed to pressurized flowing water under neutron irradiation. The results presented here may provide new insights into the performance of joining materials containing unreacted silicon proposed for SiC/SiC components in LWRs.

Due to the observed corrosion in Mo-wrap joints, the focus of the subsequent work shifted to the second pressureless joining material investigated in this study: SAY.

### 4.2. SAY

SiC samples joined using the SAY glass-ceramic remained intact after 8 h in the static autoclave (POLITO, Table I); the joints were sound, and the morphology of the SAY (not shown here) was unchanged, retaining the three crystalline phases reported in [4,6,7,16–18].

Additional SAY-joined SiC samples were tested for 14 days in the static autoclave (PARR, SCK•CEN, Table I). Even after prolonged exposure, the joints remained sound upon visual inspection (Fig. 7a, b). The lack of SAY in some parts of the joint both before (Fig. 7a) and after (Fig. 7b) testing is attributed to defects inherent to the slurry-based

**Table II**  
X-ray Computer Tomography facilities and characteristics.

Facility	Instrument	Voxel size	Key settings*
J-TECH@PoliTO Oxford University	Custom Fraunhofer IKTS (Germany) Zeiss Xradia Versa 510	5.9 $\mu\text{m}$	180 kV, 90 $\mu\text{A}$ , 1 s exposure, 0.2 mm Cu filter
		5.9 $\mu\text{m}$	70 kV, 6 W, 8 s, LE #4, 1 601 projections
		2.55 $\mu\text{m}$	80 kV, 7 W, 25 s, LE #6, 1 601 projections
		0.93 $\mu\text{m}$	130 kV, 10 W, 27 s, HE #6, 2 401 projections

(\*Exposure time refers to per-projection duration).

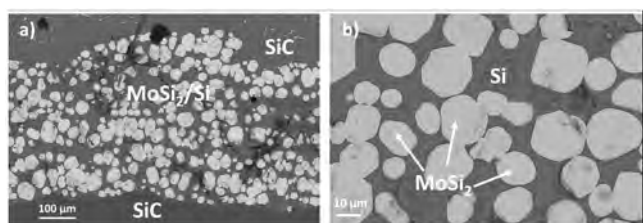


**Fig. 4.** SEM polished cross-section of a Mo-wrap joined SiC (a) and higher magnification of the joint with the  $\text{MoSi}_2$  particles well embedded in the Si matrix.

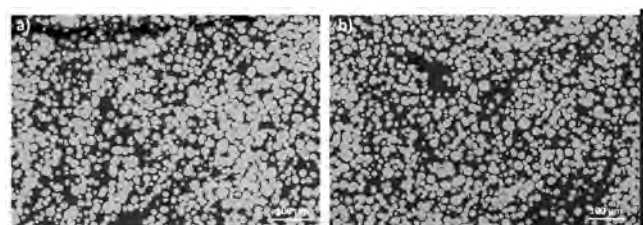


**Fig. 5.** SEM of Mo-wrap coatings on SiC before (a) and after (b) 8 h in static autoclave (POLITO, Table I) showing unchanged morphology, with  $\text{MoSi}_2$  particles well embedded in the Si matrix (top view).

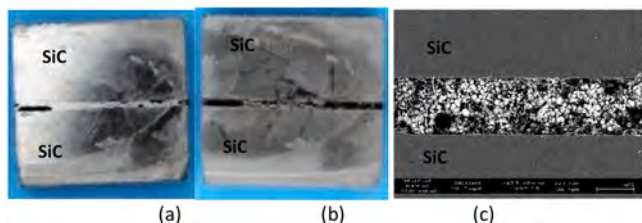


**Fig. 6.** Visual appearance of Mo-wrap joined SiC before (a) and after (b) 14 days in PARR static autoclave at SCK•CEN (Table I); SEM showing corrosion of the Si matrix in the Mo-wrap joint (c), unpolished sample.

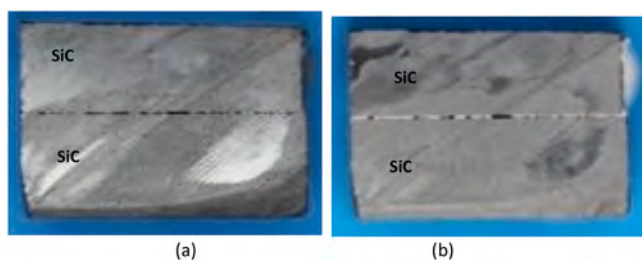


**Fig. 7.** SAY glass-ceramic joined SiC: visual appearance before (a) and after (b) 14 days in static autoclave (PARR, SCK•CEN, Table I).

joining process: the joint strength can be affected by the porosity and to overcome this issue, a different joining technology might be beneficial [10]. However, Fig. 7 shows that the autoclave exposure did not significantly affect the joint structure: the porosity visible in Fig. 7a is also present in Fig. 7b, and it does not appear to increase after the corrosion test. Additionally, Fig. 7 is a visual inspection, while the X-ray Computer Tomography in Fig. 8, gives an overview of the entire joined region and porosity.

Micro-XCT analysis of SAY-joined SiC after the 14-day autoclave test in static autoclave (PARR, SCK•CEN, Table I) (Fig. 8) confirmed the partial lack of joining material in the joined region, but the retention of the crystalline structure and the structural integrity of the joint across the full interface. Moreover, most of the pores are closed, thus not dangerous for the joint tightness.

Orthogonal slices acquired at 2.55  $\mu\text{m}$  voxel resolution (a, b) show no visible dissolution of SAY at the exposed surface, which is further corroborated by high-resolution scanning (0.93  $\mu\text{m}$  voxel, c).

SEM analysis of polished cross-sections (Fig. 9a, b) showed the expected crystalline SAY morphology. However, SEM of unpolished, as-tested surfaces (Fig. 9c, d) revealed early-stage corrosion and partial dissolution of some phases.

Encouraged by these results, SiC/SiC tubes were joined to SiC/SiC end-plugs using SAY, as shown in Fig. 10 (a–c). Two types of end-plugs were tested: Type 1 (a), a simple cylindrical shape, and Type 2 (b, c), featuring an enlarged top and a groove to serve as a slurry reservoir.

X-ray Computer Tomography in Figs. 10 (a–c) shows excellent wettability and infiltration of the SAY into the interface between tube and plug, as well as into the composite porosities. The joint thickness remained uniform, indicating that the glass-ceramic material allows controlled viscosity—an important advantage over metallic brazes, which tend to exhibit low viscosity when molten and may not provide such uniformity. Mechanical testing to compare the two end-plug geometries is currently ongoing.

Unfortunately, SAY-joined SiC samples subjected to 30-day loop autoclave tests (CORTELLINI, SCK•CEN, Table I) showed evidence of surface corrosion. In one case, complete joint failure occurred after

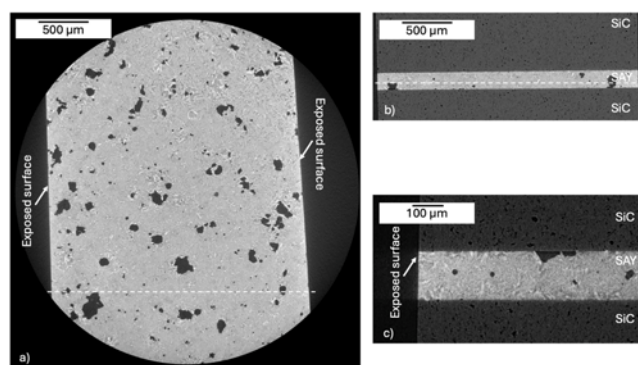


**Fig. 8.** X-ray Computer Tomography of SAY-joined SiC after static autoclave (PARR, SCK•CEN, Table I): a) and b) show orthogonal sections at 2.55  $\mu\text{m}$  voxel size (the dashed line shows the location of the respective sections); c) shows a section orthogonal to the exposed edge at 0.96  $\mu\text{m}$  voxel. (Oxford University, UK).

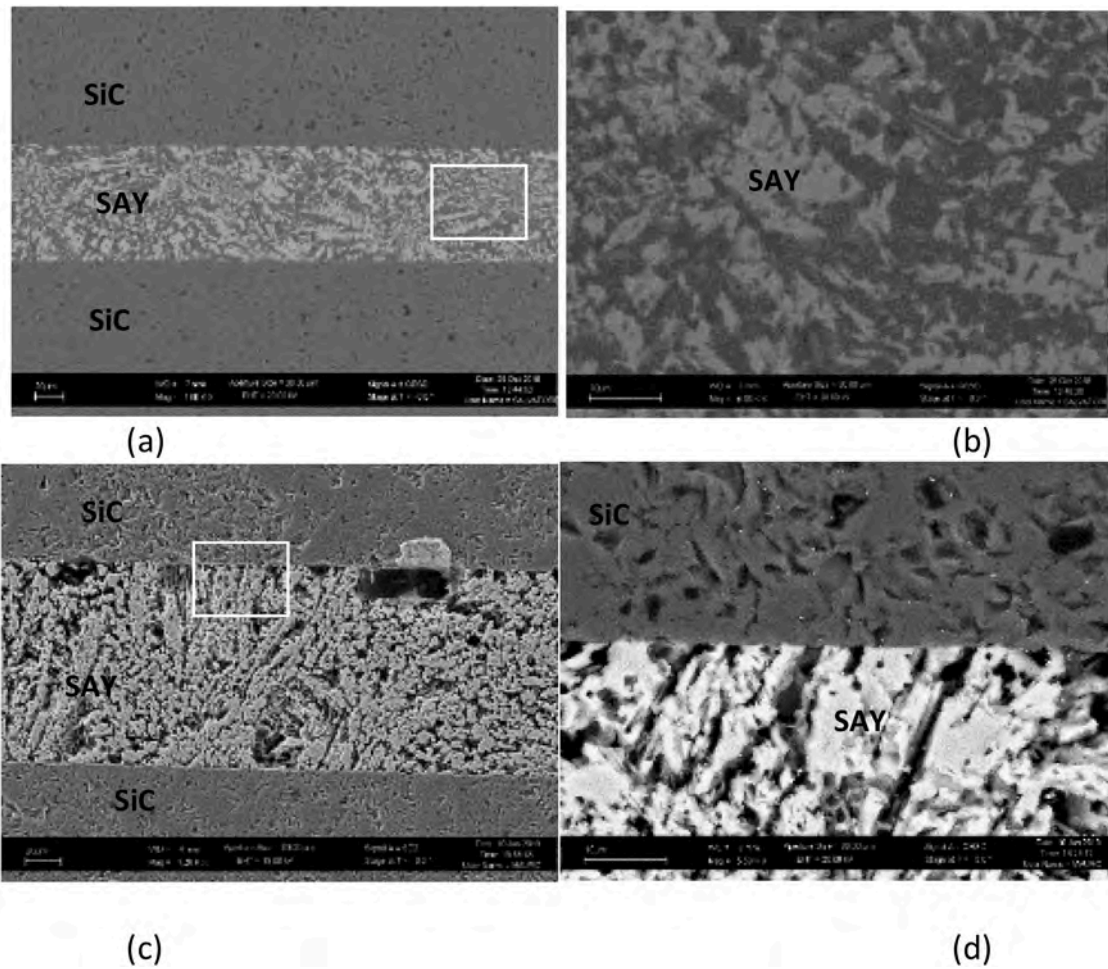


**Fig. 9.** SEM images of cross-sections of SAY-joined SiC tested in the static autoclave (PARR, SCK•CEN, Table I): (a,b) polished samples showing the non-affected SAY glass ceramic; (c,d) as-tested unpolished joint cross-sections showing a limited corrosion. (b, and d, are higher magnifications of the selected areas.).

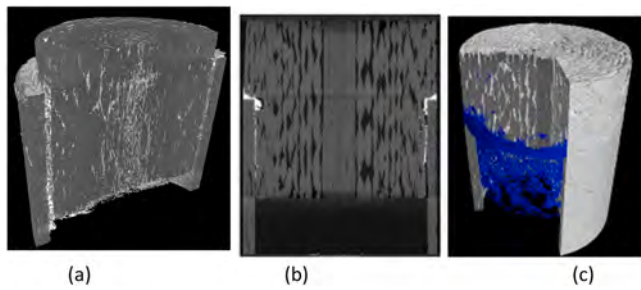


**Fig. 10.** SiC/SiC tubes joined with SAY with end plug (type 1) (a) and with modified end plug geometry (type 2) (b,c) . X-ray Computer Tomography (b,d) at J-TECH@PoliTO, Politecnico di Torino).

exposure, with visible degradation of the SAY from the perimeter toward the center of the joint (Fig. 11). SEM images show apparently distinct regions, but EDS analyses of these regions were inconclusive in identifying compositional differences.

To identify the phase(s) affected by corrosion, XRD analysis was performed on SAY fracture surfaces before and after loop autoclave exposure (Fig. 12). The comparison shows significant loss of mullite and cristobalite, with keivite ( $Y_2Si_2O_7$ ) as the main residual phase.

Additionally, SEM and EDS (Fig. 13a, b) of the remaining SAY after loop autoclave exposure confirmed the presence of Y, Si, and O, consistent with the retention of keivite, as supported by the XRD pattern in Fig. 12 (EDS data not reported here).

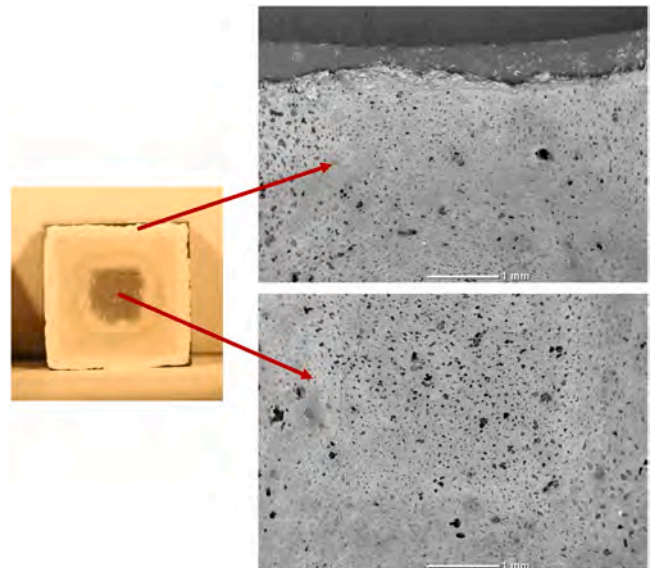


**Fig. 11.** SAY joined SiC after loop autoclave tests (CORTELINI, SCK•CEN, Table I): joints failed after test, with evident corrosion starting from the perimeter and continuing through the center of the joined region (visual inspection), and SEM of different regions as indicated.

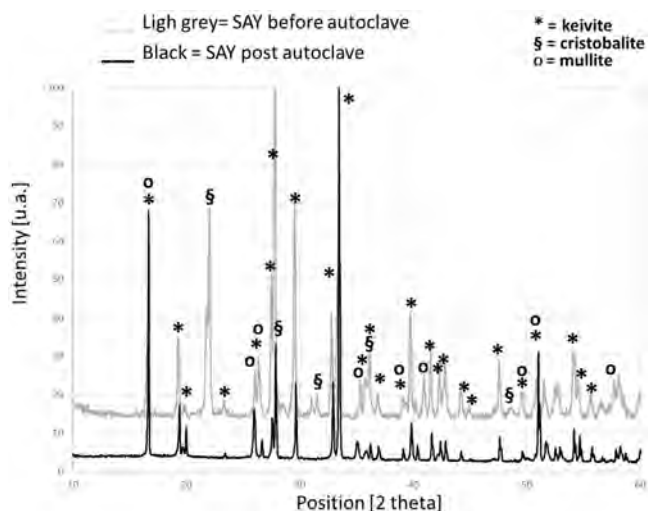


Fig. 12. XRD of SAY joined SiC (fracture surfaces) after loop autoclave tests (CORTELENI, SCK•CEN, Table I).

Similar findings have been recently reported in [28] on glasses of different compositions tested in Pressurized Water Reactor's conditions.

These findings are consistent with literature reporting higher corrosion resistance of keivite compared to silica and mullite in hydrothermal environments [26].

To investigate whether amorphous SAY joints could offer improved corrosion resistance in LWR conditions, laser joining was performed at TU Dresden. The rapid heating and cooling intrinsic to laser processing (in the order of seconds, compared to hours in a furnace) yielded a fully amorphous SAY joint (Fig. 14a, b).

Laser-joined samples were tested for 14 days in the static autoclave (PARR, SCK•CEN, Table I). Fig. 15 (a, b) shows that joints remained intact; however, higher magnification (b) revealed minor corrosion at the exposed surface.

After 30 days in the loop autoclave (CORTELENI, SCK•CEN, Table I), one of three laser-joined samples survived. Partial corrosion was observed in the amorphous SAY, originating from the exposed edge (Fig. 16a, b).

The unaffected central region remained well bonded and fully amorphous (Fig. 16c), typical of a laser joint; EDS analysis of this region confirmed retention of the original SAY composition (EDS data not reported).

## 5. Conclusions

Two pressure-less joining materials—Mo-wrap and SAY—were evaluated for sealing SiC-based components for LWR applications.

Mo-wrap joints remained mechanically sound after 14 days in static autoclave testing, but corrosion was observed, driven by dissolution of residual metallic silicon. This highlights the need for silicon-free or fully-reacted MoSi<sub>2</sub>-based fillers in LWR environments.

SAY glass-ceramic joints demonstrated good performance in static autoclave conditions (up to 14 days) and maintained a stable crystalline structure, primarily mullite, cristobalite, and keivite.

Under extended (30-day) loop autoclave conditions, SAY joints exhibited selective phase degradation, with mullite and cristobalite dissolving and keivite emerging as the dominant residual phase.

Laser-assisted joining of SiC with SAY produced fully amorphous joints, which showed improved corrosion resistance over crystalline counterparts in both static and loop autoclave tests.

These results provide valuable insights into the long-term stability of joining materials under realistic LWR conditions and guide future material selection and joint design for accident-tolerant SiC/SiC cladding systems.

## CRediT authorship contribution statement

**Monica Ferraris:** Writing – review & editing, Writing – original draft, Supervision, Funding acquisition. **Stefano De la Pierre:**

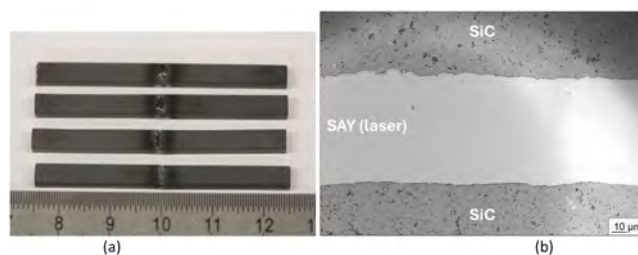


Fig. 14. SAY laser-joined SiC (TU-Dresden, Germany): visual inspection (a) and SEM (b) cross-section (b).

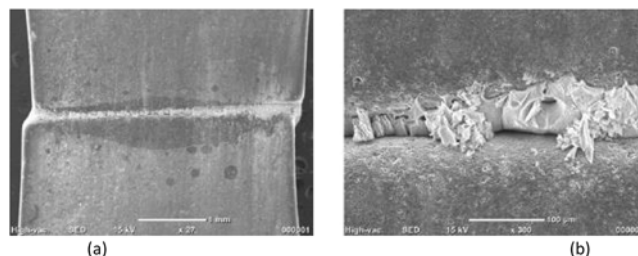


Fig. 15. SAY laser-joined SiC after static autoclave (PARR, SCK•CEN, Table I) showing a sound joint (a) and limited corrosion (b) of the amorphous SAY.

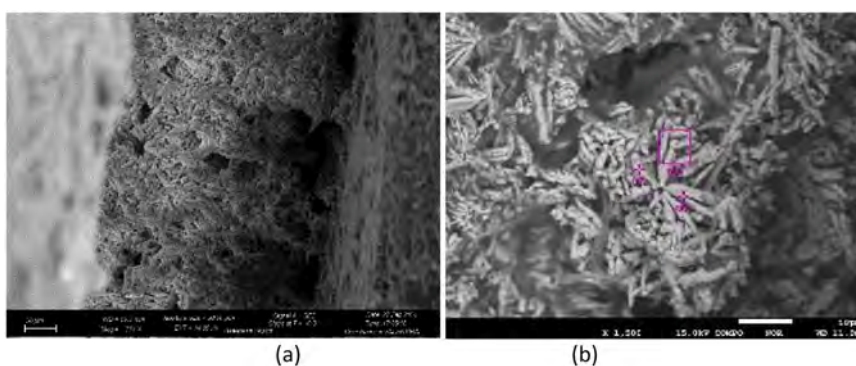
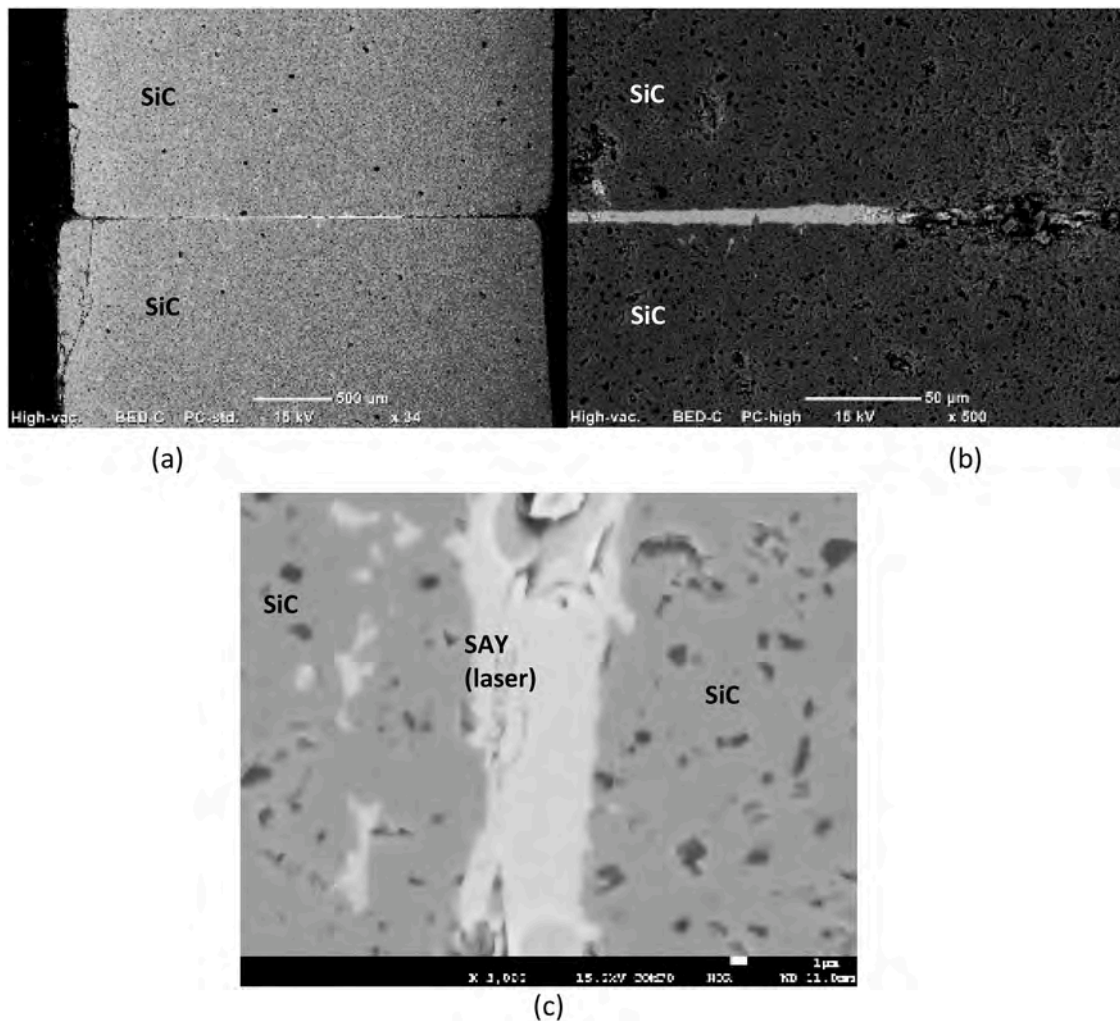


Fig. 13. SEM (a) and EDS (b) of residual SAY after loop autoclave tests (CORTELENI, SCK•CEN, Table I) (a) showing the presence of Si, Y and O only as residual elements after corrosion.



**Fig. 16.** SAY laser joined SiC (TU-Dresden) after loop autoclave (CORTELINI, SCK•CEN, Table 1) showing a partial corrosion of the joint (a,b) and the fully amorphous unaffected central region (c). EDS analysis of this region confirmed retention of the original SAY composition (EDS results not reported here).

Investigation. **Valentina Casalegno:** Investigation. **Rik-Wouter Bosch:** Investigation. **James Marrow:** Investigation. **Yang Chen:** Investigation. **Frédérique Bourlet:** Investigation. **Christophe Lorrette:** Supervision, Funding acquisition. **Shuigen Huang:** Investigation. **Konstantina Lambrinou:** Project administration.

#### Declaration of competing interest

The authors declare that they have no known competing financial interests or personal relationships that could have appeared to influence the work reported in this paper.

#### Acknowledgements

This research has received funding from the Euratom Research and Training Programme 2014–2018 under grant agreement No. 740415 (H2020 IL TROVATORE).

Dr. Marion Herrmann (TU-Dresden, Germany) is kindly acknowledged for performing laser joints and for her valuable discussions. The authors would like to thank Mr. Cédric Sauder (CEA) for carrying out the densification of the CVI-SiC/SiC composites, Prof. Luigi Manna (Politecnico di Torino) for the preliminary tests in autoclave and Koba van Loo from KU Leuven for helping out with the Parr (static) and Cortelini (loop) autoclave tests.

#### References

- [1] G.S. Was, D. Petti, S. Ukai, S. Zinkle, *Mater. Future Nucl. Energy Syst.*, *J. Nucl. Mater.* 527 (2019) 2, <https://doi.org/10.1016/j.jnucmat.2019.151837>.
- [2] K.A. Terrani, Accident tolerant fuel cladding development: promise, status, and challenges, *J. Nucl. Mater.* 501 (2018) 13–30, <https://doi.org/10.1016/j.jnucmat.2017.12.043>.
- [3] G. Liu, Z. Liu, H. Yu, X. Wang, Y. Zhou, Recent advances in joining of SiC-based materials: joining processes, joint strength, and interfacial behavior, *J. Adv. Ceram.* 8 (2019) 19–38, <https://doi.org/10.1007/s40145-018-0297-x>.
- [4] M. Ferraris, M. Salvo, V. Casalegno, A. Ciampichetti, F. Smeacetto, M. Zucchetti, Joining of machined SiC/SiC composites for thermonuclear fusion reactors, *J. Nucl. Mater.* 375 (2008) 410–415, <https://doi.org/10.1016/j.jnucmat.2008.02.020>.
- [5] T. Koyanagi, Y. Katoh, M. Ferraris, et al., Progress in development of SiC-based joints resistant to neutron irradiation, *J. Eur. Ceram. Soc.* 40 (2020) 1023–1034, <https://doi.org/10.1016/j.jeurceramsoc.2019.10.055>.
- [6] M. Ferraris, V. Casalegno, S. Rizzo, M. Salvo, T.O. Van Staveren, J. Matejcek, Effects of neutron irradiation on glass-ceramics as pressure-less joining materials for SiC based components for nuclear applications, *J. Nucl. Mater.* 429 (2012) 166–172, <https://doi.org/10.1016/j.jnucmat.2012.05.035>.
- [7] L. Gozzelino, V. Casalegno, G. Ghigo, T. Moskalewicz, A. Czyska-Filemonowicz, M. Ferraris, He-irradiation effects on glass-ceramics for joining of SiC-based materials, *J. Nucl. Mater.* 472 (2016) 28–34, <https://doi.org/10.1016/j.jnucmat.2016.01.024>.
- [8] T. Koyanagi, et al., Irradiation resistance of silicon carbide joint at light water reactor-relevant temperature, *J. Nucl. Mater.* 488 (2017) 150–159, <https://doi.org/10.1016/j.jnucmat.2017.03.017>.
- [9] T. Koyanagi, et al., Hydrothermal corrosion of silicon carbide joints without radiation, *J. Nucl. Mater.* 481 (2016) 226–233, <https://doi.org/10.1016/j.jnucmat.2016.09.027>.
- [10] M. Ferraris, M. De Maddis, D. Basile, K. Aliev, D. Alidoost, A. Benelli, S. De La Pierre, V. Casalegno, M. Herrmann, S. Huang, J. Vleugels, C. Lorrette, C. Sauder,

- K. Lambrinou, Laser assisted joining of SiC/SiC for nuclear applications, *Open Ceram* 23 (2025) 100802, <https://doi.org/10.1016/j.oceram.2025.100802>.
- [11] <https://www.ga.com/ga-achieves-another-milestone-in-silicon-carbide-composite-nuclear-fuel-rod-technology> (2025) (visited on June 24, 2025).
- [12] P.K. Gianchandani, V. Casalegno, F. Smeacetto, M. Ferraris, Pressure-less joining of C/SiC and SiC/SiC by a MoSi<sub>2</sub>/Si composite, *Int. J. Appl. Ceram. Technol.* 14 (2017) 305–312, <https://doi.org/10.1111/ijac.12631>.
- [13] P.K. Gianchandani, V. Casalegno, M. Salvo, M. Ferraris, I. Dlouhý, Refractory Metal, RM-Wrap: a tailorable, pressure-less joining technology, *Ceram. Int.* 45 (2019) 4824–4834, <https://doi.org/10.1016/j.ceramint.2018.11.178>.
- [14] P.K. Gianchandani, V. Casalegno, M. Salvo, G. Bianchi, A. Ortona, M. Ferraris, SiC foam sandwich structures obtained by Mo-wrap joining, *Mater. Lett.* 221 (2018) 240–243, <https://doi.org/10.1016/j.matlet.2018.03.105>.
- [15] P.K. Gianchandani, V. Casalegno, S. De La Pierre des Ambrois, M. Salvo, G. De Aloysio, L. Laghi, M. Ferraris, Joining of SiC, alumina and mullite by the Refractory Metal (RM) – Wrap pressure-less process, *Int. J. Appl. Ceram. Technol.* (2020), <https://doi.org/10.1111/ijac.13477>.
- [16] F. Smeacetto, M. Ferraris, M. Salvo, S.D. Ellacott, A. Ahmed, R.D. Rawlings, et al., Protective coatings for carbon bonded carbon fibre composites, *Ceram. Int.* 34 (2008) 1297–1301, <https://doi.org/10.1016/j.ceramint.2007.03.012>.
- [17] F. Smeacetto, M. Salvo, M. Ferraris, V. Casalegno, G. Canavese, T. Moskalewicz, et al., Erosion protective coatings for low density, highly porous carbon/carbon composites, *Carbon*. N. Y. 47 (2009) 1511–1519, <https://doi.org/10.1016/j.carbon.2009.01.045>.
- [18] M. Ferraris, M. Salvo, V. Casalegno, S. Han, Y. Katoh, H.C. Jung, et al., Joining of SiC-based materials for nuclear energy applications, *J. Nucl. Mater.* 417 (2011) 379–382, <https://doi.org/10.1016/j.jnucmat.2010.12.160>.
- [19] J. Braun, et al., Influence of an original manufacturing process on the properties and microstructure of SiC/SiC tubular composites, *Compos. A* 123 (2019) 170–179, <https://doi.org/10.1016/j.compositesa.2019.04.031>.
- [20] C. Morel, et al., The influence of internal defects on the mechanical behavior of filament wound SiC/SiC composite tubes under uniaxial tension, *J. Eur. Ceram. Soc.* 43 (2023) 1797–1807, <https://doi.org/10.1016/j.jeurceramsoc.2022.12.040>.
- [21] C. Morel, et al., The influence of grinding process on the mechanical behavior of SiC/SiC composite tubes under uniaxial tension, *J. Eur. Ceram. Soc.* 44 (2023) 91–106, <https://doi.org/10.1016/j.jeurceramsoc.2023.07.067>.
- [22] M. Herrmann, W. Lippmann, A. Hurtado, High-temperature stability of laser-joined silicon carbide components, *J. Nucl. Mater.* 443 (2013) 458–466, <https://doi.org/10.1016/j.jnucmat.2013.07.067>.
- [23] M. Herrmann, W. Lippmann, A. Hurtado, Y<sub>2</sub>O<sub>3</sub>-Al<sub>2</sub>O<sub>3</sub>-SiO<sub>2</sub>-based glass-ceramic fillers for the laser-supported joining of SiC, *J. Eur. Ceram. Soc.* 34 (2014) 1935–1948, <https://doi.org/10.1016/j.jeurceramsoc.2014.01.019>.
- [24] M. Herrmann, S. Ahmad, W. Lippmann, H.J. Seifert, A. Hurtado, Rare earth aluminosilicates for the joining of silicon carbide components, *Int. J. Appl. Ceram. Technol.* 14 (2017) 675–691, <https://doi.org/10.1111/ijac.12692>.
- [25] W. Lippmann, M. Herrmann, A. Hurtado, Laser joining of silicon carbide – a new technology for ultra-high temperature resistant joint, *Nucl. Eng. Des* 231 (2004) 151–161, <https://doi.org/10.1016/j.nucengdes.2004.03.002>.
- [26] R.-W. Bosch (2024), SCK•CEN, private communication, unpublished results from II Trovatore project, report D5.1.
- [27] H. Kishimoto, J.-S. Park, N. Nakazato, A. Kohyama, Silicon dissolution and morphology modification of NITE SiC/SiC claddings in pressurized flowing water under neutron irradiation, *J. Nucl. Mater.* 557 (2021) 153221, <https://doi.org/10.1016/j.jnucmat.2021.153253>.
- [28] S. Yang, X. Liu, C. Liang, J. Li, Y. Ma, S. Kou, et al., Enhanced hydrothermalcorrosion resistance in SiC/SiC joints with CaO-modified Y-Al-Si-O interlayer under PWR condition, *J. Am. Ceram. Soc.* 108 (2025) e70119, <https://doi.org/10.1111/jace.70119>.